Properties of L-Type Calcium Channel Gating Current in Isolated Guinea Pig Ventricular Myocytes

ROBERT W. HADLEY and W. J. LEDERER

From the Department of Physiology, School of Medicine, University of Maryland at Baltimore, Baltimore, Maryland 21201

ABSTRACT Nonlinear capacitative current (charge movement) was compared to the Ca current (I_{Ca}) in single guinea pig ventricular myocytes. It was concluded that the charge movement seen with depolarizing test steps from −50 mV is dominated by L-type Ca channel gating current, because of the following observations. (*a*) Ca channel inactivation and the immobilization of the gating current had similar voltage and time dependencies. The degree of channel inactivation was directly proportional to the amount of charge immobilization, unlike what has been reported for Na channels. (*b*) The degree of Ca channel activation was closely correlated with the amount of charge moved at all test potentials between −40 and +60 mV. (*c*) D600 was found to reduce the gating current in a voltage- and use-dependent manner. D600 was also found to induce "extra" charge movement at negative potentials. (*d*) Nitrendipine reduced the gating current in a voltage-dependent manner (K_D = 200 nM at −40 mV). However, nitrendipine did not increase charge movement at negative test potentials. Although contamination of the Ca channel gating current from other sources cannot be fully excluded, it was not evident in the data and would appear to be small. However, it was noted that the amount of Ca channel gating charge was quite large compared with the magnitude of the Ca current. Indeed, the gating current was found to be a significant contaminant (19 ± 7%) of the Ca tail currents in these cells. In addition, it was found that Ca channel rundown did not diminish the gating current. These results suggest that Ca channels can be "inactivated" by means that do not affect the voltage sensor.

INTRODUCTION

The Ca current (I_{Ca}) has been regarded to have a number of vital yet disparate roles in cardiac tissues, including a contribution to diastolic depolarization (Noma et al., 1980), maintenance of the action potential plateau (Reuter and Scholz, 1977), and both stimulation of release and replenishment of internal Ca stores (Fabiato, 1985). This has stimulated considerable interest in cardiac Ca channels, and cardiac ventricular myocytes have become a common model preparation for studying the

Address reprint requests to Dr. Robert W. Hadley, Department of Physiology, University of Maryland School of Medicine, 655 West Baltimore Street, Baltimore, MD 21201.

J. GEN. PHYSIOL. © The Rockefeller University Press · 0022-1295/91/08/0265/21 $2.00
Volume 98 August 1991 265–285

basic properties of Ca channels (cf. Lee and Tsien, 1982; Cavalie et al., 1983; Nilius et al., 1985). One means of investigating Ca channels that has not been widely used is the study of gating currents, although such experiments have proven to be key to understanding Na channel function (Armstrong, 1981). Ca channel gating currents have been reported in molluscan neurons (Adams and Gage, 1979; Kostyuk et al., 1981) and in scorpion skeletal muscle (Scheuer and Gilly, 1986). It has also been argued that, in vertebrate skeletal muscle, the dihydropyridine-sensitive portion of charge movement that is usually thought to control Ca release from the sarcoplasmic reticulum (Rios and Brum, 1987), may be more directly related to Ca channel gating (Lamb and Walsh, 1987).

Intramembrane charge movement had not been studied in heart until quite recently. Perhaps not surprisingly, Na channel gating current has been identified as a prominent feature of cells isolated from Purkinje fibers (Hanck et al., 1990). The general properties of charge movement also have been studied in neonatal rat ventricular cells, where it has been suggested that Na channel gating may make less of a contribution than Ca channel gating (Field et al., 1988). Charge movement in adult ventricle has been studied in isolated rabbit, rat, and guinea pig myocytes, and has been found to be quite similar among species, with ~11–12 nC/μF of movable charge (Bean and Rios, 1989; Hadley and Lederer, 1989*a*). The charge movement in these cells has been suggested to consist of two major components, since charge immobilization was found to have a biphasic dependence on membrane potential (Bean and Rios, 1989; Hadley and Lederer, 1989*a*). The two phases of charge immobilization seemed to approximately correspond to the known voltage dependence of Na and Ca channel inactivation, suggesting that gating currents from these channels may account for the two components of cardiac charge movement. Although the general characterization of cardiac charge movement has proven useful, more detailed studies are necessary if the study of gating currents is to prove useful in understanding cardiac calcium channels. In particular, it is necessary to isolate, to as great an extent as possible, the Ca channel gating current, and to appraise the extent to which Na channel gating current contaminates the recordings. Such contamination may prove troublesome, as it has been demonstrated that even when Na channels are completely inactivated by a depolarizing prepulse, the immobilization of the Na channel gating charge is incomplete (Armstrong and Bezanilla, 1977; Hanck et al., 1989). Although recent studies (Field et al., 1988; Bean and Rios, 1989) have provided evidence that the behavior of much of the charge movement under study is consistent with Ca channel gating, the amount of contribution made by Na channel gating remains uncertain. In the present experiments, the Ca channel gating current was investigated by applying test pulses from holding potentials positive to −50 mV (without a prepulse to more negative potentials). The charge movement studied under these conditions appeared to be almost entirely Ca channel gating current, as it was possible to demonstrate a linear relationship between the amount of charge moved and the degree of Ca channel activation. Thus, the recordings appear to be dominated by Ca channel gating current with negligible contamination from Na channel gating. This approach to the investigation of cardiac Ca channels provided new information on various aspects of Ca channel function, including inactivation, rundown, and dihydropyridine block.

A preliminary report on some of these experiments has been published (Hadley and Lederer, 1989*b*).

METHODS

Cell Preparation

All of the experiments were performed with single cardiac ventricular myocytes isolated from adult guinea pigs (250–400 g) of either sex. The procedure was a standard one originally described by Mitra and Morad (1985), where the myocytes are enzymatically dispersed by retrograde perfusion through the aorta of collagenase- and protease-containing solutions. The animals were anesthetized with pentobarbital before dissection. Further details were previously described (Hadley and Lederer, 1989*a*).

Solutions

Table I gives the composition of the major external solutions that were used. Minor modifications of these solutions, such as concentration changes, will be noted in the figure

TABLE I

Composition of External Solutions

	NaCl	KCl	$CaCl_2$	$MgCl_2$	CsCl	$CdCl_2$	$LaCl_3$	NMDG-Cl
					mM			
120 Na, 2.5 Ca	120	4	2.5	1.0	20	—	—	—
0 Na, 2 Cd	—	—	1.0	1.0	—	2	0.1	145
20 Na	20	4	1.0	1.0	20	—	0.1	105
0 Na, 5 Ca	—	—	5.0	1.0	—	—	—	145
4 Mg	—	—	—	4.0	—	—	—	145

All external solutions also contained 10 mM glucose and 10 mM HEPES. All external solutions except the 20 Na solution contained 0.03 mM tetrodotoxin.

legends. The standard pipette solution contained (in millimolar): Cs glutamate 110, tetraethylammonium Cl 20, CsCl 20, *N*-2-hydroxyethylpiperazine-*N'*-2-ethanesulfonic acid (HEPES) 10, ethyleneglycol-bis(β-aminoethyl ether)-*N,N'*-tetraacetic acid (EGTA) 1, and Mg adenosine triphosphate (ATP) 2. All solutions were adjusted to pH 7.4 using NaOH or CsOH if the primary cation was Na or Cs, respectively, or with HCl when *N*-methyl-D-glucamine (NMDG) was the primary cation. A junction potential of −12 mV was present after zeroing the pipette potential in the bath, and was corrected for in the experiments. All of the experiments were done at 20–22°C.

General Procedures

The myocytes were voltage-clamped with the whole-cell patch clamp technique (Hamill et al., 1981). Pipette resistances ranged from 0.2 to 2 MΩ when filled with the standard pipette solution. An Axopatch 1-C patch clamp amplifier with a CV-3 0.1 headstage (Axon Instruments, Inc., Burlingame, CA) was used to voltage-clamp the cells. Series resistance compensation was used in most of the experiments. Current records were low-pass filtered with a cutoff frequency of 2–10 kHz.

Data Analysis

Current and voltage records were digitized with a sampling frequency of 5–10 kHz, and stored on an IBM PC-AT (IBM Instruments, Inc., Danbury, CT) for analysis. They were also simultaneously digitized at 11 kHz, and stored on a videocassette recorder for permanent storage. Charge movement records were constructed by adding the test record (produced by a depolarization from the holding potential) to the control record. The control record was usually produced by a single hyperpolarization from −100 to −140 mV, and the record was scaled up to match the amplitude of the test pulse. Control records were taken repeatedly during the experiment, usually just before or after each test step. The repeated estimates of linear capacitance were taken to compensate for slow changes in the time course of the capacitative transient. The gain of the system was kept low to prevent saturation of the amplifiers, which introduced bit noise into the records. The noise was also enhanced during the scaleup of the control record. On occasion, when the noise was especially deleterious, the control record was fit with an exponential function, and this was used for the construction of the charge movement records. The amount of charge moved was calculated by defining the steady-state current level as the baseline, and integrating the current over the time of the test step. The steady-state current level was defined as the current mean over the last few milliseconds of the test step. Kinetic data were fit to exponential functions on a 80386 microcomputer using the program "Kinfit" (On-Line Instrument Systems, Inc., Jefferson, GA), which utilized the Marquardt algorithm. Variation in the data is displayed as standard errors.

Voltage-Clamp Protocol

The protocol used to "isolate" the supposed L-type Ca channel gating current was simple. Test depolarizations were imposed from a holding potential of −50 mV, but only after the holding potential had been maintained at −50 mV for at least several seconds. Linear capacitance was then estimated for the subtraction procedure by shifting the holding potential to −100 mV. After waiting several seconds, a hyperpolarization to −140 mV was given. (See Hadley and Lederer [1989*a*] for an evaluation of the method used for subtracting linear capacitance.) The intention of this protocol was to separate, to as great an extent as possible, a large portion of the Ca channel gating current from other sources of charge movement. An important aim of this study was to evaluate to what extent this was true.

RESULTS

Comparison of Charge Movement and Ca Channel Activation

As mentioned in the Introduction, charge movement in adult guinea pig ventricular myocytes seems to consist of two major components, which are roughly separated by a holding potential of −50 mV. The principal interest of these studies was to test the correlation of the second charge movement component to the gating of L-type Ca channels. It has been suggested that the two charge components may be roughly separated using a holding potential of −50 mV (Bean and Rios, 1989; Hadley and Lederer, 1989*a*). Therefore, the second charge component was measured as that produced by depolarization from a holding potential no more negative than −50 mV.

If the second charge movement component is actually a Ca channel gating current, it must be able to account for I_{Ca} activation. Fig. 1 shows two current records obtained in the same cell. The first record was obtained in 0 Na, 5 Ca external solution (and is

labeled as such), which isolated I_{Ca} from other membrane currents. The second record was obtained shortly afterwards in 0 Na, 4 Cd solution, which blocked ionic currents and allowed measurement of charge movement. It can be seen that during a voltage-step from −50 to +10 mV in the 0 Na, 5 Ca solution, a rapid outward current was present before I_{Ca} began to dominate the recording. I_{Ca} peaks by the end of the 6-ms step, and then a tail current is seen upon repolarization. The charge movement record consists of an outward current transient during the depolarization (Q_{on}), and an inward transient during the repolarization (Q_{off}).

Comparison of the two records reveals several points. First, the outward current seen before I_{Ca} seems to be Q_{on}. Second, the Q_{on} transient approaches its steady-state level by the time I_{Ca} reaches its peak. Third, the declining phases of the I_{Ca} tail and the Q_{off} transient have about the same time course. The time constants were 0.65 ms for the tail current, and 0.77 ms for Q_{off}. Although the kinetics have not been rigorously examined by varying the test and repolarization potentials, qualitatively,

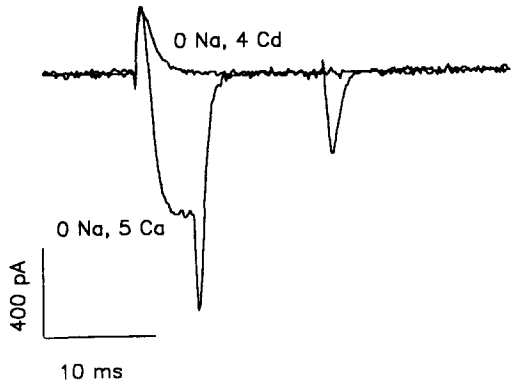

FIGURE 1. Comparison of I_{Ca} and charge movement kinetics. The traces show current records obtained in 0 Na, 5 Ca external solution and 0 Na, 4 Cd solution. The test step consisted of either a 6- or 20-ms depolarization from −50 to +10 mV. A 6-ms step was used to study I_{Ca} to produce maximal activation, yet avoid rapid Ca-dependent inactivation. A 20-ms step was used to study charge movement, in order to get a good baseline for evaluating Q_{on}. Q_{on} was 293 fC and Q_{off} was −285 fC in the 0 Na, 4 Cd solution. Linear capacitance was subtracted off using a hyperpolarization from −100 to −140 mV for both records. The capacitative transient decayed with a time constant of 0.28 ms (0 Na, 5 Ca) or 0.26 ms (0 Na, 4 Cd). Cell capacitance was 63 pF.

this charge movement component is rapid enough to at least be consistent with I_{Ca} activation and deactivation. A final point of interest is the large size of the charge movement transients relative to I_{Ca}.

This last point is further emphasized in Fig. 2*A*. The figure plots tail current measurements in another guinea pig ventricular cell. The voltage-clamp protocol consisted of a 7-ms step from −50 mV to the potential indicated on the *x*-axis. The resulting tail currents were measured in 0 Na, 5 Ca solution (○), or 0 Na, 4 Cd solution (●). The unfilled circles are the usual measurements of I_{Ca} tail currents. However, it is obvious from Fig. 1 that these tail currents also contain current due to the Q_{off} transient. When the peak Q_{off} currents are measured separately, the difference current, representing current actually carried by Ca influx, can be calculated (△). It is evident that the standard "Ca tail currents" can be heavily contaminated by charge movement. However, the proportion varies widely among

five cells (0.19 ± 0.07, range 0.07–0.39), largely depending on the amount of Ca influx that was present.

It is apparent from Fig. 2 *A* that although the Q_{off} transients can produce a significant error in the measurement of the absolute magnitude of Ca tail currents, relative measurements would be much less affected. This is because the voltage dependence of both the Ca tail current and the Q_{off} transients are quite comparable. This is shown more clearly in Fig. 2 *B*, where the average Ca channel conductance calculated from the "true" tail currents (○) and the integrated charge during the Q_{on}

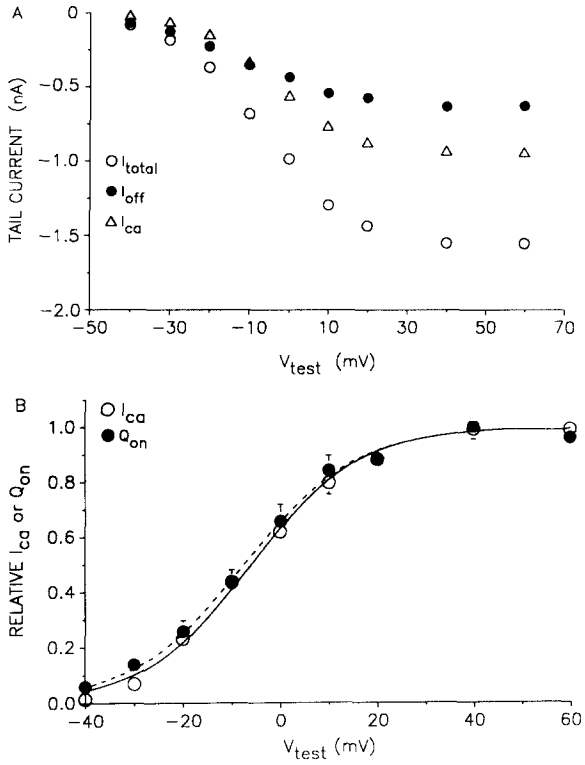

FIGURE 2. Voltage dependence of charge movement and I_{Ca} activation. (*A*) An example of the voltage dependence of different tail current components in a ventricular myocyte. The voltage-clamp protocol was a 7-ms step from −50 mV to the potentials indicated on the abscissa. In 0 Na, 5 Ca solution this procedure measured the total tail current (○). The magnitude of the Q_{off} tail currents was measured in 0 Na, 4 Cd solution (●). The difference current (△) represents the true I_{Ca}. (*B*) Normalized conductance–voltage relationship for I_{Ca} (○) and the charge–voltage relationship for Q_{on} (●). The voltage-clamp protocol was the same as in *A*. The solid curve is a Boltzmann fit to the I_{Ca} data, where V^* was −6 mV, and k was 11 mV. The dashed curve is a fit to the Q_{on} data, where V^* was −7.5 mV, and k was 11.5 mV. Error bars for the I_{Ca} data are down, whereas the error bars for the Q_{on} data are up. Error bars were not shown when they were smaller than the data symbols. Cell capacitance was 50 pF. n = 5 cells.

transient (●) are plotted against the test potential. The voltage dependence of both I_{Ca} and Q_{on} almost overlap, indicating that Q_{on} can account for I_{Ca} activation.

Ca Channel Inactivation and Charge Immobilization

Fig. 3 shows statistics for a detailed comparison of Ca channel inactivation and charge movement immobilization. Panel *A* plots the voltage dependence of I_{Ca} inactivation (●) and charge immobilization (○) over a broad range of potentials. The voltage-clamp protocol was the same for both measurements; a 500-ms prepulse

was given from −50 mV to various potentials, and after a 10-ms interval, a 20-ms test step was given from −50 to 0 mV. Direct comparison of the two sets of data is complicated by the fact that there are two mechanisms for Ca channel inactivation in cardiac tissue: voltage-dependent and Ca-dependent inactivation (Kass and Sanguinetti, 1984; Lee et al., 1985; Hadley and Hume, 1987). The immobilization of a supposed Ca channel gating current would of course only be due to voltage-dependent inactivation, as charge movement is measured in the absence of ionic current. However, the degree of charge immobilization and I_{Ca} inactivation are quite

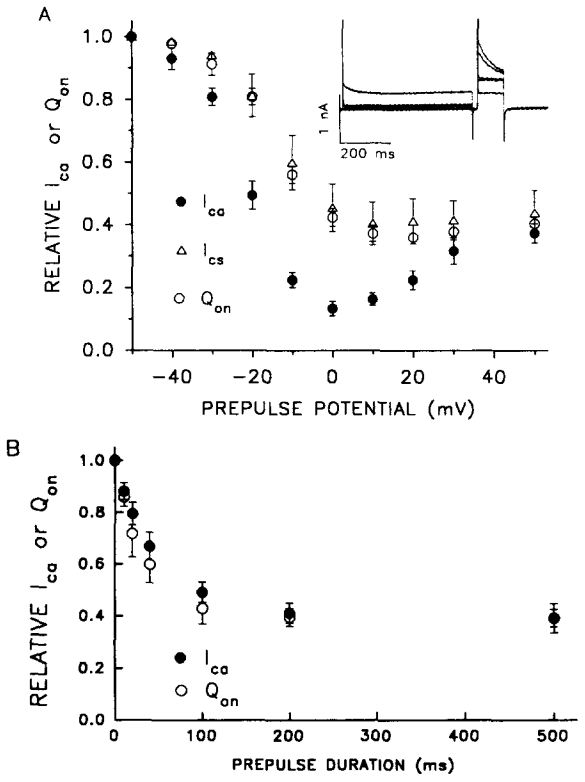

FIGURE 3. Comparisons of Ca channel inactivation and charge immobilization. Total Ca channel inactivation, voltage-dependent inactivation, and charge immobilization were evaluated in the 120 Na-2.5 Ca, 4 Mg, and 0 Na-2 Cd external solutions, respectively. Data were pooled from five cells for all three conditions, and are plotted in *A*. The voltage-clamp protocol consisted of a 500-ms prepulse from −50 mV to a variable potential, which was followed by a test step after a 10-ms interval at −50 mV. The test step was set to 0 mV for the I_{Ca} and Q_{on} measurements, and +90 mV for the I_{Cs} measurements. Current records from one I_{Cs} experiment are shown in the *inset*. I_{Cs} during the second, test pulse decreases as the prepulse potential is changed to (in sequence) −50, −20, 0, and +50 mV. The smallest outward current is seen after the addition of Cd. *B* compares the kinetics of I_{Ca} inactivation and charge immobilization. The voltage clamp protocol was the same as in *A*, except the prepulse potential was fixed at +50 mV, and the duration was varied instead. n = 4 cells.

similar at positive potentials where there is less Ca influx. Nevertheless, it would be useful to compare charge immobilization only with voltage-dependent inactivation, and over a less restricted range of membrane potentials. This was accomplished by another set of experiments done in the 4 Mg external solution. This solution was designed to be quite similar to that used to measure charge movement, except that Ca and the inorganic Ca channel blockers were replaced with Mg. The advantage of this solution is that there is no ion capable of carrying a significant inward current through Ca channels, but permits Cs to carry an outward current through the

channels. I_{Cs} was measured with a 100-ms test step to +90 mV, and Cd-insensitive leak current was subtracted off (an example of the current records are shown as the *inset* in *A*). The results from these experiments are plotted in Fig. 3 *A* as the triangles, and demonstrate that voltage-dependent Ca channel inactivation has the same voltage dependence as charge immobilization.

Panel *B* compares the kinetics of I_{Ca} inactivation and charge immobilization. A variable duration prepulse was given to +50 mV, and then after a 10-ms interval at −50 mV, a test step was given to 0 mV. The prepulse was set at +50 mV to minimize Ca-dependent inactivation. It is obvious that at +50 mV, I_{Ca} inactivation and charge immobilization are comparable in both extent and time course.

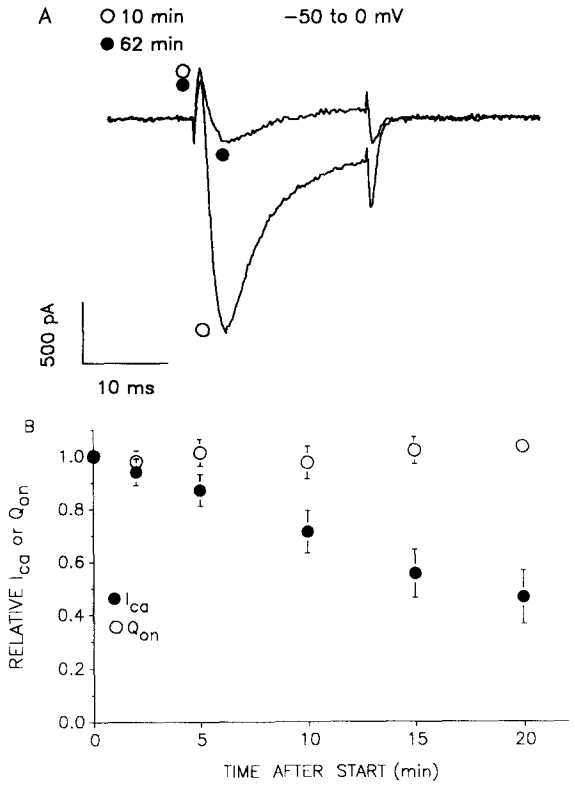

FIGURE 4. Stability of I_{Ca} and charge movement. (*A*) Records obtained in 0 Na, 3 Ca external solution, with a 20-ms step from −50 to 0 mV. Linear capacitance was subtracted off. Both traces are labeled with the time during the experiment that they were obtained. (*B*) Plots of accumulated data, where either I_{Ca} (●) or Q_{on} (○) were monitored over time. Both sets of data were gathered separately from five cells each. The means were significantly different at 15 and 20 min, as judged by a one-tailed Student's *t* test ($P = 0.05$).

Stability of I_{Ca} and Charge Movement

Although the experiments described to this point indicate a close correlation of the second charge movement component and Ca channel gating, Fig. 4 demonstrates one difference. Panel *A* shows current records (after linear capacitance subtraction) obtained in 0 Na, 3 Ca solution. The records were obtained at different times after access to the cell interior was obtained (indicated next to the traces). It can be seen that over the course of 1 h, I_{Ca} in this cell ran down considerably, but the outward

current representing Q_{on} was considerably less affected. However, this is not a clear comparison, as the Q_{on} peak could be affected by the activation of I_{Ca}. A comparison of the stability of I_{Ca} and Q_{on} is hard to do quantitatively, as monitoring both currents in the same cell requires repetitive washing of Cd ions on and off the cell. It then becomes fairly uncertain whether I_{Ca} is diminished because of rundown, or partial block by Cd. However, the stability of the two can be compared in separate cells. Panel *B* plots data gathered from separate sets of cells where either I_{Ca} (●) or Q_{on} (○) was monitored. I_{Ca} ran down continuously over the course of an experiment, whereas Q_{on} rarely showed any sign of decrease. These results could be taken as demonstrating dissociation between this charge movement component and I_{Ca}. However, it can also be interpreted as indicating that the mechanism of Ca channel rundown involves regions of the channel not associated with sensing the membrane potential. The merit of each of these hypotheses will be elaborated on in the Discussion.

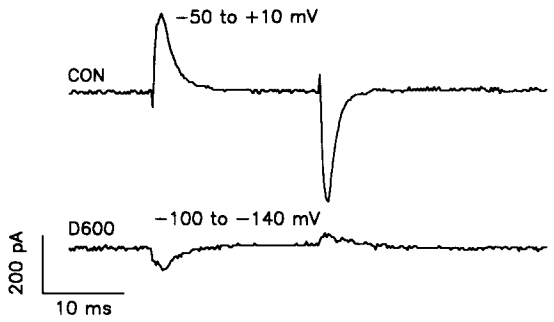

FIGURE 5. D600 induces excess charge movement at negative potentials. The bottom trace shows charge movement that occurred with a step from −100 to −140 mV, the normal "control" for estimating linear capacitance. The control for this record was a hyperpolarization from −140 to −180 mV, obtained after remaining at −140 mV for 30 s. The upper trace shows the charge moved under control conditions, with a test step from −50 to +10 mV, in order to compare the magnitudes.

Pharmacology of the Putative Ca Channel Gating Current

The effect of certain Ca channel blockers on charge movement was also studied. When D600 was first applied to ventricular myocytes, it was found to have complicated effects. For example, D600 (10 μM) was found to increase the amount of charge moved during the usual control hyperpolarization (from −100 to −140 mV). This is shown in Fig. 5. The lower trace is a charge movement record obtained by a hyperpolarization from the holding potential of −100 to −140 mV in the presence of the drug. In order to show this effect another control pulse protocol had to be found that was not altered by the drug. The new control procedure consisted of a hyperpolarization from −140 to −180 mV, after the cell had remained at −140 mV for at least 30 s. The absolute amount of charge moved during the drug-free hyperpolarization (−100 to −140 mV) was 2,189 fC. The control record in D600 (−140 to −180 mV) was 2,175 fC. In the presence of D600, a hyperpolarization from −100 to −140 mV moved 2,266 fC. The amount of "extra" charge moved between −100 and −140 mV in the presence of D600 is large enough to seriously mar charge movement records, if this were to be used as a control record. In order to permit

ready comparison of the amount of "extra" charge produced by D600, the top trace of Fig. 5 shows a charge movement record obtained under control conditions. Similar observations were made in four other cells. The nature of this "extra" charge movement at negative potentials has not been examined, but may be related to the recovery of ionic channels from D600 block. All of the D600 experiments were done with the type of control described for this experiment.

D600 also affects charge movement seen with depolarizations. Fig. 6*A* shows charge movement records before and after application of 10 μM D600. The records

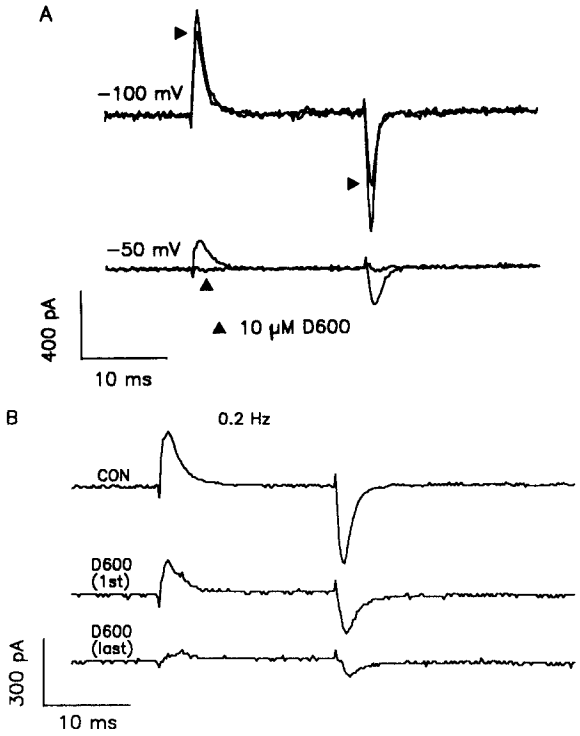

FIGURE 6. D600 inhibition of charge movement. The top traces of *A* show the steady-state effect of 10 μM D600 on charge movement evoked by a step from −100 to +10 mV. D600 somewhat reduced both Q_{on} and Q_{off}, as indicated by the arrows. The bottom traces show that D600 can inhibit all of the charge movement seen from a holding potential of −50 mV. The absolute amount of charge moved during the drug-free control was 2,183 fC, and was 2,202 fC during the control in D600. *B* demonstrates that the decrease of charge movement associated with Ca channel gating is use dependent. The top trace shows charge movement during a 20-ms step from −50 to +10 mV under control conditions. The middle record was obtained with the first stimulation after applying 10 μM D600, and the bottom record was obtained after 1 min of 0.2-Hz stimulation. The absolute amount of charge moved during the drug-free control was 2,189 fC, and was 2,175 fC in the control used for the D600 traces. Same cell as in Fig. 5.

were produced by 20 ms steps from the holding potential (indicated on the figure) to +10 mV. It was necessary to repetitively stimulate the cells in order to see an effect of D600. This was done by running a 1-min train (at 0.33 Hz) of 200 ms pulses from the holding potential to +10 mV, before giving the test pulse. It can be seen that D600 reduced both Q_{on} and Q_{off} at a holding potential of −100 mV. However, the effect of D600 was voltage dependent, as the same concentration of D600 inhibited essentially all of the charge movement at a holding potential of −50 mV. The average reduction of Q_{on} by D600 when the effect was at steady state was 19 ± 6% at −100 mV, and 100 ± 5% at −50 mV (n = 5).

D600 inhibition was also use dependent, as suggested by the need for the loading trains in the above experiments. Use-dependent inhibition by D600 is demonstrated in Fig. 6 *B*. The top trace is a charge movement record obtained during a train of voltage-clamp steps from −50 to +10 mV, at 0.2 Hz. Repetitive stimulation at this rate had little effect on charge movement under control conditions. Stimulation of the cell was then halted, and 10 μM D600 applied. The middle trace shows charge movement obtained by the first depolarization after resuming stimulation, and the bottom trace shows charge movement after 1 min of stimulation. Clearly, reduction of charge movement by D600 becomes more pronounced with repetitive stimulation. Similar results were seen in three other cells. These results are in full agreement with a prior report of use-dependent inhibition of cardiac charge movement by D600 (Bean and Rios, 1989), although the effect of D600 during hyperpolarizations has not been previously reported in heart cells. A component of skeletal muscle charge movement is also sensitive to D600 (Hui et al., 1984). In summary, the decrease of charge movement by D600 is voltage- and use-dependent, and 10 μM D600 can inhibit all of the charge movement component associated with Ca channel gating (holding potential of −50 mV). These characteristics closely resemble D600 block of Ca channels (McDonald et al., 1984; Uehara and Hume, 1985).

The effect of nitrendipine, a dihydropyridine Ca channel blocker, on charge movement was also examined. Fig. 7 *A* displays representative charge movement records obtained before and after applying 200 nM nitrendipine. The effect of nitrendipine was strongly voltage dependent, as it did not decrease charge movement seen with a voltage step to +10 mV given directly from the holding potential of −100 mV (top trace), but completely inhibited charge movement seen with a voltage step from −30 to +10 mV (bottom trace). No previous stimulation was necessary to produce the decrease. Fig. 7 *B* plots the average effect of nitrendipine on charge movement at different holding potentials between −50 and −20 mV. Again, the inhibition is strongly voltage dependent, but not strongly use-dependent. These properties correspond to what has been described for dihydropyridine block of Ca channels (Sanguinetti and Kass, 1984; Uehara and Hume, 1985).

As it has been reported that dihydropyridines increase the amount of charge moved at negative potentials in skeletal muscle (Rios and Brum, 1987), it could be argued that the effect seen here with depolarizations could be complicated by drug effects on the control hyperpolarization. An increase in the charge moved during the control step, for example, could cause an artificial decrease in the charge movement seen with the test step. Although the cells remained at −100 mV for several seconds before giving the control step, it was still necessary to check for this effect. Table II shows the effect of different concentrations of nitrendipine on the absolute amount of charge moved during the control hyperpolarization. The drug effects were measured during the first control step after returning from −40 mV. Thus, any effect of the drug should be prominent. However, there was no significant difference at any drug concentration, and certainly no hint of an increase. Therefore, the nitrendipine effects seen in Fig. 7 cannot be ascribed to artifact.

The experiments shown in Table II were also designed to measure the dose-dependence of the inhibitory effects of nitrendipine at a holding potential of −40 mV. (The test step was to +10 mV.) These data are shown in Fig. 8, and are

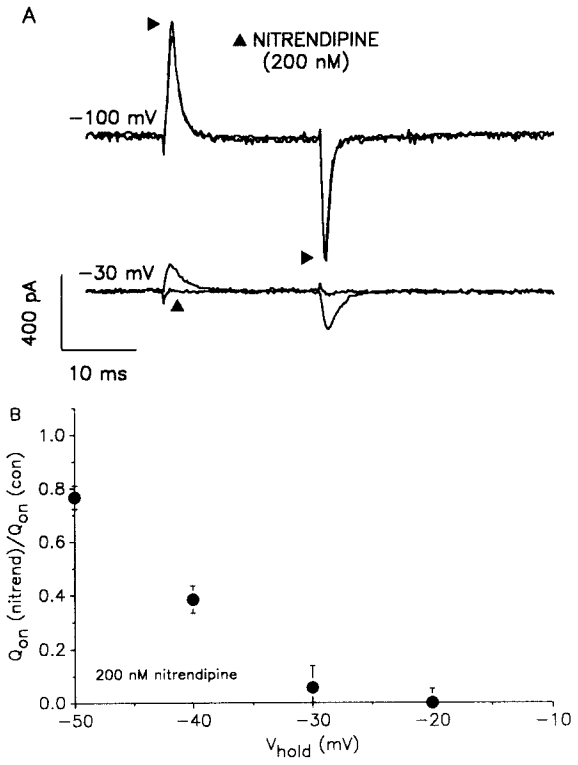

FIGURE 7. Dihydropyridine inhibition of Ca channel gating current. (*A*) Charge movement records obtained in the absence and presence of 200 nM nitrendipine (arrows) at two holding potentials. The 20-ms test step to +10 mV was given directly from the indicated holding potentials. (*B*) Variation of the amount of inhibition according to holding potential. Voltage-clamp protocol was the same as before. n = 5 cells.

reasonably well fit by a 1:1 drug–receptor binding curve with a K_D of 200 nM. Also note that the data do not reveal any obvious dihydropyridine-resistant component. These data are in good agreement with that reported for nitrendipine block of cardiac I_{Ca}. Lee and Tsien (1983) reported a K_D of 154 nM at −40 mV, while Sanguinetti and Kass (1984) reported that 200 nM nitrendipine blocked 51–56% of

TABLE II

Effect of Nitrendipine on Control Hyperpolarization

Nitrendipine	Relative capacitance	SE	n
nM			
20	0.994	0.0087	5
67	0.986	0.0086	5
200	0.997	0.0049	5
670	0.994	0.0068	4
2,000	0.977	0.015	4

The tabulated data show the lack of effect of nitrendipine on the control hyperpolarizations (a step from −100 to −140 mV), under the conditions used in this study. Capacitance was calculated as the average of Q_{on} and Q_{off}. After application of the drug, the cell capacitance was measured after returning from a holding potential of −40 mV, which should have exacerbated any drug effect. The data were normalized relative to the cell capacitance before drug application (measured using the same protocol).

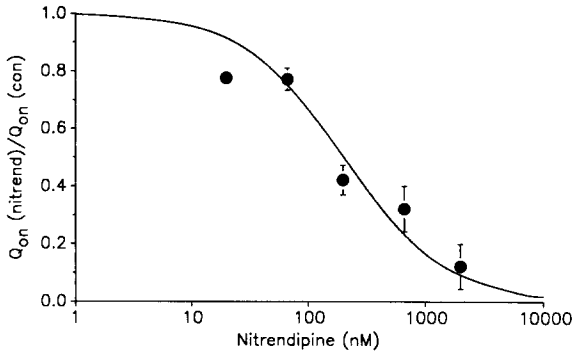

FIGURE 8. Dose dependence of the reduction of gating current by nitrendipine. This figure plots the average decrease of Q_{on} by various concentrations of nitrendipine. The holding potential was −40 mV, and the test potential was +10 mV. The curve shows the least-squares fit of a theoretical curve to the data, assuming 1:1 drug–receptor binding. The K_D for nitrendipine was 200 nM. Mean values were calculated from four to five cells for each data point. The data were derived from the same experiments as in Table II.

I_{Ca} at a holding potential of −45 mV. The second component of charge movement is therefore not only closely correlated to the functional aspects of Ca channel function, but also shares much of its pharmacology.

Although the data presented so far have demonstrated a close correspondence of the Ca channel gating current to known Ca channel properties, it was still necessary to further evaluate possible contamination of the measurements by Na channel gating charge. Fig. 9 shows a comparison of the effects of nitrendipine (1 μM) on I_{Na} (*A*) and the Ca channel gating current (*B*). It can be seen that the same concentration

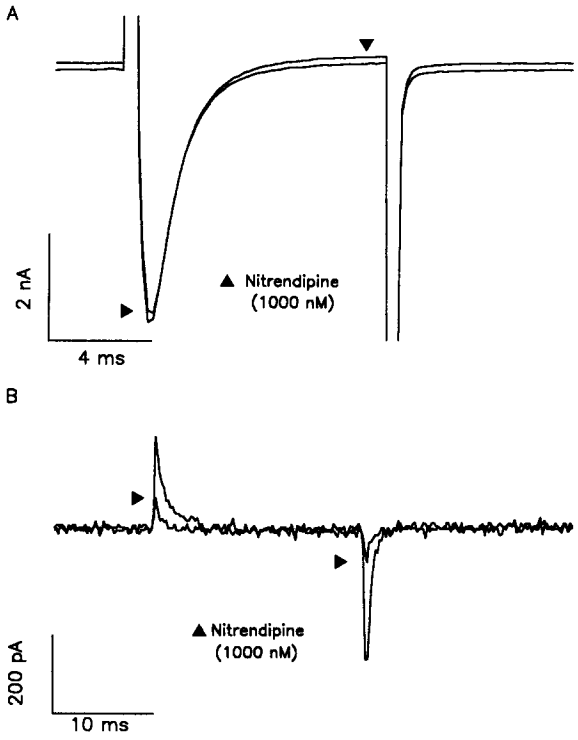

FIGURE 9. Comparison of the effect of nitrendipine on I_{Na} and gating current. (*A*) I_{Na} records obtained in 20 Na external solution, before and after application of 1 μM nitrendipine. The holding potential was −40 mV. I_{Na} was measured by first giving a 200-ms prepulse to −80 mV, which was followed by a 10-ms test step to −20 mV. (*B*) Gating current records obtained from a different cell in 0 Na, 2 Cd solution using a 20-ms test step from −40 to +10 mV.

of nitrendipine can almost completely inhibit the gating current while producing minimal effects on I_{Na}. I_{Na} in the presence of nitrendipine was 0.96 ± 0.07 of control values.

DISCUSSION

Identification of L-type Ca Channel Gating Current

The major conclusion of this paper is that the charge moved with depolarizations from −50 mV in guinea pig ventricular myocytes is predominantly L-type Ca channel gating current. This conclusion was reached because of the close correspondence between the voltage dependence of charge movement and I_{Ca} activation, the similarities between the voltage dependence and kinetics of charge movement and I_{Ca} inactivation, and the finding that two classes of Ca channel antagonists act on charge movement in a manner analogous to Ca channel blockade. Although other membrane proteins would be expected to move in response to changes in the membrane potential, their contribution to the second component of charge movement seems to be minimal, since the Ca conductance– and charge–voltage curves (Fig. 2 *B*) almost overlap. Most surprising about the predominance of Ca channel gating current is the apparently small contribution from Na channel gating current, which was directly demonstrated by comparing the dihydropyridine sensitivity of I_{Na} and the Ca channel gating current. Na channels would be completely inactivated at the holding potential of −50 mV, but Na channel inactivation only immobilizes roughly two-thirds of the gating charge (Armstrong and Bezanilla, 1977; Nonner, 1980; Hanck et al., 1989). Why doesn't this nonimmobilized fraction, which should still be sizable, mar the recordings of Ca channel gating current? The answer is not entirely clear, but it may be because the cells were held at −50 mV for many seconds. The Na channel gating current would first be reduced by the usual inactivation process, and also some amount of the gating charge would already have moved by −50 mV. It may also be possible that slow inactivation of Na channels (Chandler and Meves, 1970) further reduces the Na channel gating current to the point where it is dwarfed by the Ca channel gating current. Thus, although the voltage-clamp protocol might not be expected to eliminate Na channel gating charge, it apparently reduces it to the point where it is obscured by Ca channel gating.

It should be noted that little evidence has been found in this study to support a significant contribution of inwardly rectifying K channels to Q_{off} (Bean and Rios, 1989). The size of Q_{off} was always observed to be equivalent to Q_{on}, and Q_{off} appears to have the same sensitivity to dihydropyridines as Q_{on} (Fig. 7 A). However, the voltage and time dependence of activation of the inwardly rectifying K channels is very sensitive to the concentration of permeating cations (Kurachi, 1985; Harvey and Ten Eick, 1988; Cohen et al., 1989), and it may be difficult to predict their behavior under conditions when there is little or no permeation.

It is important at this point to note the advantages and disadvantages of this approach to measurement of cardiac Ca channel gating current. The principal problem in measuring this current is to adequately separate it from other charge movements, notably that due to Na channel gating. Other investigators have examined cardiac charge movement and its correlation with Ca channel gating by

giving test steps from around −100 mV (Field et al., 1988; Bean and Rios, 1989). In the current experiments, the cell was not briefly returned to −100 mV before the test step, because of concerns that the considerable Na channel gating charge might rapidly become reavailable and be seen during the test step. Thus, as mentioned in the previous paragraph, this may account for the fact that the residual Na channel gating current is obscured by the Ca channel gating current, and the latter can be studied in relative isolation. However, this approach has a limitation in that any Ca channel gating that occurs at potentials negative to −50 mV is lost. The amount of lost gating charge would appear to be small, as the gating charge seen under these conditions is as large, or larger than in the other reports. The amount of Ca channel gating charge was estimated to be 5.0 nC/μF under these conditions (Hadley and Lederer, 1989*a*), compared to 6 nC/μF in adult rat or rabbit ventricular myocytes (Bean and Rios, 1989), or 3.9 nC/μF in neonatal rat ventricular myocytes (Field et al., 1988). The small amount of lost charge may reflect movement of the channel between closed states, as the remaining gating current is linearly related to Ca channel activation. The ability to study a fairly clean Ca channel gating current makes possible a number of experiments, particularly those examining the effect of certain modulators on the voltage sensor. However, alternative protocols may be better used to examine Ca channel gating that occurs negative to −50 mV.

Properties of the Ca Channel Gating Current

The immobilization of the Ca channel gating current was found to closely resemble voltage-dependent Ca channel inactivation between −50 mV and +50 mV. Since Ca influx is blocked during the charge movement measurements, it is not yet known whether Ca-dependent inactivation also immobilizes the gating charge. Further experiments on this question may provide some insight into how the two inactivation processes act on the Ca channel.

It is interesting to compare the results in Fig. 3 *A* to what is known about Na channel inactivation. Voltage-dependent inactivation of Na and Ca channels appear to have a number of similarities. Inactivation of both channels seems to be accompanied by immobilization of the charge responsible for activation. Moreover, in both channel types, very positive potentials only immobilize roughly two-thirds of the gating charge. However, there appears to be a critical difference in how charge immobilization and inactivation are coupled in Na and Ca channels. While in Na channels, partial charge immobilization leads to complete channel inactivation (Armstrong and Bezanilla, 1977; Nonner, 1980), the amount of Ca channel inactivation appears to be proportional to the degree of charge immobilization (Fig. 3 *B*). This may indicate that the failure of I_{Ca} to completely inactivate at positive potentials may be due to some divergence in the immobilization-inactivation coupling.

The close correspondence of the Ca gating current to Ca conductance (Fig. 2 *B*) also deserves comment. Field et al. (1988) along with Bean and Rios (1989) have reported that cardiac charge movement that may be associated with Ca channel gating is shifted somewhat more negative than Ca channel conductance. Fig. 2 *B* demonstrates a tight correspondence between the gating current and Ca channel conductance, but nevertheless does not contradict these other reports, as gating charge moved before −50 mV would not be detected.

Ca Channel Rundown

In this study, it was found that although I_{Ca} steadily diminished over the time of an experiment, the gating current did not. A similar phenomenon has been reported for Ca channels in *Aplysia* neurones (Kostyuk et al., 1981), and was thought to occur in rabbit and rat ventricular myocytes (Bean and Rios, 1989). As mentioned previously, this could be interpreted as meaning that this charge movement component is not L-type Ca channel gating current. However, as summarized above, other evidence strongly supports the idea that it is a Ca channel gating current, and other sources of charge movement would have to constitute the majority of gating charge to undermine this observation. Therefore, it can be postulated that this dissociation between Ca channel permeation and gating reflects the mechanism by which these Ca channels run down. It has been suggested that irreversible Ca channel rundown is due to proteolysis of the Ca channel (Chad and Eckert, 1986). If this is true, the present evidence indicates that the proteolytic damage must be fairly limited, perhaps just in the immediate vicinity of the pore mouth. Such limited degradation must lead to a small conformational change, which is enough to permanently close the pore at some point, but without profoundly affecting the voltage-sensing region of the protein. This would leave a "senescent" channel, capable of generating gating current, but not capable of permitting Ca influx.

Excess Dihydropyridine Receptors

It was obvious from the results presented in this report that the Ca channel gating current was exceptionally large compared to the magnitude of I_{Ca}. The amount of Ca channel gating charge in guinea pig ventricular myocytes was previously estimated to be 5.0 nC/μF of cell capacitance (Hadley and Lederer, 1989*a*), which is about 10-fold greater than expected from the estimated channel density of three to five channels per square micrometer of surface membrane (McDonald et al., 1986). The gating charge estimate depended upon obtaining a reasonable separation of Na and Ca channel gating currents at a holding potential of −50 mV. The present results indicate that the separation of gating currents by holding potential was appropriate. A similar discrepancy has also been reported in rabbit and rat ventricular myocytes (Bean and Rios, 1989). What does this excess of gating charge mean? It has been shown that all of the charge is correlated with Ca channel gating, and that it is sensitive to dihydropyridines. It therefore seems to arise from a relatively homogenous population of dihydropyridine receptors. This excess of gating charge requires a large majority of the receptors to sense the membrane potential, and thus generate a gating current, but not to permit Ca influx. This idea is supported by the data on Ca channel rundown, which suggest that Ca channels do supply gating current independent of whether or not they can carry Ca. The density of dihydropyridine receptors has also been measured in guinea pig ventricular myocytes using ligand binding (Kamp et al., 1988), and the density (60 receptors per square micrometer) is considerably higher than the previously estimated Ca channel density. This excess of cardiac dihydropyridine receptors somewhat resembles the situation in skeletal muscle, where it has been reported that there are 230 dihydropyridine receptors per square micrometer and 35–50 times fewer calcium channels (Schwartz et al., 1985;

but see Lamb and Walsh, 1987). In contrast, the amount of gating current seems to be in better agreement with the number of Ca channels in molluscan neurons (Kostyuk et al., 1981) and in scorpion skeletal muscle (Scheuer and Gilly, 1986).

What could be the function of the excess dihydropyridine receptors? One possibility, as suggested by the experiments on rundown, is that they are senescent (nonfunctional) Ca channels, possibly arising from partial proteolysis of the channel protein. Another possibility is that the excess number of dihydropyridine receptors are dephosphorylated Ca channels, or other dormant channels that are still capable of regaining functionality. A third possibility is that the excess dihydropyridine receptors are vestigial remnants of a voltage-dependent excitation–contraction (E-C) coupling mechanism. That is, if E-C coupling is indeed only controlled through Ca-induced Ca release, the large number of sarcolemmal voltage sensors required for voltage-dependent E-C coupling may still be there, but are simply not associated with the sarcoplasmic reticulum. The present data do not allow any of these possibilities to be excluded.

Action of Ca Channel Blockers

In this study, the actions of the calcium channel blockers D600 and nitrendipine were used to support the identification of a Ca channel gating current. In addition, D600 was found to induce extra charge movement at negative potentials, whereas nitrendipine did not. It is possible that this charge movement reflect recovery of ionic channels from block. If this is correct, the difference between the two drugs might be explained as being due to the fact that dihydropyridine unblock can occur over an order of magnitude faster than D600 unblock (Uehara and Hume, 1985). It would be expected that all of the channels blocked by nitrendipine would recover during the relatively long period (several seconds) the cell was held at −100 mV, before the control hyperpolarization was given. This would not be true for D600-blocked channels, and therefore channel recovery may have still been occurring during the control hyperpolarization.

A review of other reports in the literature reveals that a similar effect of D600 has been reported for frog skeletal muscle charge movement, at negative potentials (Melzer and Pohl, 1987). However, nifedipine has also been reported to increase charge movement at negative potentials in frog skeletal muscle (Rios and Brum, 1987) and in neonatal rat ventricular cells (Field et al., 1988). It seems likely that the difference between these reports and the present results with nitrendipine, is due to relatively slow recovery of skeletal muscle charge movement (Brum and Rios, 1987), and to the longer equilibration period at −100 mV in the present study. Field et al. (1988) also reported that 10 μM nifedipine did not decrease Q_{on} at a holding potential of −100 mV. This is in agreement with the data presented in Fig. 7, where 200 nM nitrendipine had little effect on Q_{on} at −100 mV. Field et al. did note an incongruity in the effects of nifedipine, as the same concentration of the drug blocked the majority of I_{Ca}. This might be attributed to rapid open channel block during the 20-ms depolarization, as they did note a drug-induced slowing of Q_{off}. However, other studies indicate that dihydropyridine block is much slower than this (Sanguinetti and Kass, 1984; Cohen and McCarthy, 1987). Alternatively, it could be envisioned that blocked channels still undergo most of the state transitions that give

rise to charge movement, but perhaps pass rapidly to an inactivated state (Field et al., 1988). However, the present results indicate that dihydropyridines can completely inhibit the gating current at less negative holding potentials. Field et al. did not explore the effect of nifedipine at these holding potentials, as such protocols also altered their control records.

A final point can be made that concerns the mechanism of action of the dihydropyridines. Dihydropyridine block of Ca channels has usually been viewed in terms of the modulated receptor hypothesis (Bean, 1984; Sanguinetti and Kass, 1984; Uehara and Hume, 1985), that was originally developed to explain local anesthetic block of Na channels. However, the present results point out one important difference between the two classes of drugs. Work in squid axons has demonstrated that QX-314, a quaternary lidocaine derivative, produces full Na channel block while only immobilizing a fraction of the gating charge (Cahalan and Almers, 1979). The maximal amount of gating charge that can be immobilized by QX-314 is the same amount as can be immobilized by voltage, leading to the suggestion that a drug-associated channel is functionally equivalent to an inactivated channel (Cahalan and Almers, 1979; Tanguy and Yeh, 1989). Nitrendipine block of Ca channels is somewhat different. High concentrations of the drug immobilize essentially all of the Ca channel gating charge. This difference between nitrendipine and QX-314 is consistent with the prior observations on voltage-induced charge immobilization. That is, both voltage and QX-314 immobilize a fraction of the Na channel gating charge while closing all of the channels, whereas nitrendipine and voltage seem to close Ca channels in direct proportion to their effect on gating charge. However, nitrendipine is far more efficacious than voltage, in that it immobilizes gating charge that apparently would never have been immobilized by voltage. These data not only indicate fundamental differences between Na and Ca channel inactivation, but suggest new insights into the molecular mechanism of dihydropyridine block. Dihydropyridine block has often been viewed as resulting from the drug-induced stabilization of channels that have inactivated by themselves. However, it has been pointed out that the calcium current in anterior pituitary cells is dihydropyridine-sensitive, even though inactivation is minimal (Cohen and McCarthy, 1987). The present data suggest that these results can be reconciled. In particular, the data suggest the specific hypothesis that dihydropyridines "mimic" the inactivation process when they bind to a channel, rather than simply binding to and stabilizing previously inactivated channels. A drug-associated channel behaves in much the same way as an inactivated one, but the actual binding of the drug to the channel may not depend on the channel state as strictly as previously thought. However, the voltage-dependence of dihydropyridine block does require that the closed states furthest removed from channel opening bind dihydropyridines less avidly.

Relevance of Charge Movement to Ca Current Measurements

As described in Results, the Ca channel gating current in guinea pig ventricular myocytes is sizable, considering the magnitude of I_{Ca}. Although linear leak and capacitative currents are routinely subtracted from I_{Ca} records, most studies have not reported the large Q_{on} transient seen just before the activation of I_{Ca}. This can

probably be attributed to inaccurate estimates of linear capacitance, done over a voltage range where Na channels were gating.

The finding that "Ca tail currents" contain much current due to Q_{off} deserves further comment. This indicates that ignoring the gating current introduces a significant error in the actual tail current measurements, but the effect on relative measurements is smaller, since the voltage dependence of I_{Ca} and the Ca channel gating current is the same. These errors will be reduced or accentuated under different experimental conditions. First, it is obvious that since Ca channel rundown affects I_{Ca}, but not the gating current, heavy rundown of I_{Ca} will increase the error. Furthermore, the proportion of gating current to the actual Ca tail current will change over time. Secondly, the measurement error can be diminished by increasing the driving force for Ca across the membrane. Elevation of the external Ca concentration is the simplest way to do this, although care must be taken that voltage control is not affected. Ca influx during the tail could also be enhanced by repolarization to more negative potentials. However, the Na channel gating current may then begin to contaminate the recordings. This new error might also greatly affect relative conductance measurements.

We would like to thank Cecilia Neubauer for assistance in figure preparation.

This research was supported by National Institutes of Health grants HL-25675 and HL-36974. Dr. Hadley is supported by the Sarnoff Research Fellowship of the Maryland Heart Association.

Original version received 8 December 1989 and accepted version received 20 March 1991.

REFERENCES

Adams, D. J., and P. W. Gage. 1979. Sodium and calcium gating currents in an *Aplysia* neurone. *Journal of Physiology.* 291:467–481.

Armstrong, C. M. 1981. Sodium channels and gating currents. *Physiological Reviews.* 61:644–683.

Armstrong, C. M., and F. Bezanilla. 1977. Inactivation of the sodium channel. *Journal of General Physiology.* 70:567–590.

Bean, B. P. 1984. Nitrendipine block of cardiac calcium channels: high-affinity binding to the inactivated state. *Proceedings of the National Academy of Sciences.* 81:6388–6392.

Bean, B. P., and E. Rios. 1989. Non-linear charge movement in the membranes of mammalian cardiac ventricular cells: components from Na and Ca channel gating. *Journal of General Physiology.* 94:65–93.

Brum, G., and E. Rios. 1987. Intramembrane charge movement in frog skeletal muscle fibres: properties of charge 2. *Journal of Physiology.* 387:489–517.

Cahalan, M. D., and W. Almers. Interactions between quaternary lidocaine, the sodium channel gates, and tetrodotoxin. *Biophysical Journal.* 27:39–56.

Cavali, A., R. Ochi, D. Pelzer, and W. Trautwein. 1983. Elementary currents through Ca^{2+} channels in guinea-pig myocytes. *Pflügers Archiv.* 398:284–297.

Chad, J. E., and R. Eckert. 1986. An enzymatic mechanism for calcium current inactivation in dialyzed *Helix* neurones. *Journal of Physiology.* 378:31–51.

Chandler, W. K., and H. Meves. 1970. Slow changes in membrane permeability and long-lasting action potentials in axons perfused with fluoride solutions. *Journal of Physiology.* 211:707–728.

Cohen, C. J., and R. T. McCarthy. 1987. Nimodipine block of calcium channels in rat anterior pituitary cells. *Journal of Physiology.* 387:195–225.

Cohen, I. S., D. DiFrancesco, N. K. Mulrine, and P. Pennefather. 1989. Internal and external K^+ help gate the inward rectifier. *Biophysical Journal.* 55:197–202.

Fabiato, A. 1985. Simulated calcium current can both cause calcium loading in and trigger calcium release from the sarcoplasmic reticulum of a skinned canine cardiac Purkinje cell. *Journal of General Physiology.* 85:291–320.

Field, A. C., C. Hill, and G. D. Lamb. 1988. Asymmetric charge movement and calcium currents in ventricular myocytes of neonatal rat. *Journal of Physiology.* 406:277–297.

Hadley, R. W., and J. R. Hume. 1987. An intrinsic potential-dependent inactivation mechanism associated with calcium channels in guinea-pig myocytes. *Journal of Physiology.* 389:205–222.

Hadley, R. W., and W. J. Lederer. 1989*a*. Intramembrane charge movement in guinea-pig and rat ventricular myocytes. *Journal of Physiology.* 415:601–624.

Hadley, R. W., and W. J. Lederer. 1989*b*. L-type calcium channel gating current in isolated guinea-pig ventricular myocytes. *Journal of Physiology.* 418:27P. (Abstr.)

Hamill, O. P., A. Marty, E. Neher, B. Sakmann, and F. Sigworth. 1981. Improved patch-clamp techniques for high-resolution current recording from cells and cell-free membrane patches. *Pflügers Archiv.* 391:85–100.

Hanck, D. A., M. F. Sheets, and H. A. Fozzard. 1989. Immobilization of Na channel gating current in single canine purkinje cells. *Biophysical Journal.* 55:317*a*. (Abstr.)

Hanck, D. A., M. F. Sheets, and H. A. Fozzard. 1990. Gating currents associated with Na channels in canine cardiac Purkinje cells. *Journal of General Physiology.* 95:439–457.

Harvey, R. D., and R. E. Ten Eick. 1988. Characterization of the inward-rectifying potassium current in cat ventricular myocytes. *Journal of General Physiology.* 91:593–615.

Hui, C. S., R. L. Milton, and R. S. Eisenberg. 1984. Charge movement in skeletal muscle fibers paralyzed by the calcium-entry blocker D600. *Proceedings of the National Academy of Sciences.* 81:2582–2585.

Kamp, T. J., M. C. Sanguinetti, and R. J. Miller. 1988. Voltage-dependent binding of dihydropyridine calcium channel blockers to guinea pig ventricular myocytes. *Journal of Pharmacology and Experimental Therapeutics.* 247:1240–1247.

Kass, R. S., and M. C. Sanguinetti. 1984. Inactivation of calcium channel current in the calf cardiac Purkinje fiber: evidence for voltage- and calcium-mediated mechanisms. *Journal of General Physiology.* 84:705–726.

Kostyuk, P. G., O. A. Krishtal, and V. I. Pidoplichko. 1981. Calcium inward current and related charge movements in the membrane of snail neurones. *Journal of Physiology.* 310:403–421.

Kurachi, Y. 1985. Voltage-dependent activation of the inward-rectifier potassium channel in the ventricular cell membrane of guinea-pig heart. *Journal of Physiology.* 366:365–385.

Lamb, G. D., and T. Walsh. 1987. Calcium currents, charge movement and dihydropyridine binding in fast- and slow-twitch muscles of rat and rabbit. *Journal of Physiology.* 393:595–617.

Lee, K. S., E. Marban, and R. W. Tsien. 1985. Inactivation of calcium channels in mammalian heart cells: joint dependence on membrane potential and intracellular calcium. *Journal of Physiology.* 364:395–411.

Lee, K. S., and R. W. Tsien. 1982. Reversal of current through calcium channels in dialyzed single heart cells. *Nature.* 297:498–501.

Lee, K. S., and R. W. Tsien. 1983. Mechanism of calcium channel blockade by verapamil, D600, diltiazem and nitrendipine in single dialyzed heart cells. *Nature.* 302:790–794.

McDonald, T. F., A. Cavalie, W. Trautwein, and D. Pelzer. 1986. Voltage-dependent properties of macroscopic and elementary calcium channel currents in guinea pig ventricular myocytes. *Pflügers Archiv.* 406:437–448.

McDonald, T. F., D. Pelzer, and W. Trautwein. 1984. Cat ventricular muscle treated with D600: characteristics of calcium channel block and unblock. *Journal of Physiology.* 352:217–241.

Melzer, W., and B. Pohl. 1987. Effects of D600 on the voltage sensor for Ca release in skeletal muscle fibres of the frog. *Journal of Physiology.* 390:151P. (Abstr.)

Mitra, R., and M. Morad. 1985. A uniform enzymatic method for dissociation of myocytes from hearts and stomachs of vertebrates. *American Journal of Physiology.* 249:H1056–H1060.

Nilius, B., P. Hess, J. B. Lansman, and R. W. Tsien. 1985. A novel type of cardiac calcium channel in ventricular cells. *Nature.* 316:443–446.

Noma, A., H. Kotake, and H. Irisawa. 1980. Slow inward current and its role mediating the chronotropic effect of epinephrine in the rabbit sinoatrial node. *Pflügers Archiv.* 388:1–9.

Nonner, W. 1980. Relations between the inactivation of sodium channels and the immobilization of gating charge in frog myelinated nerve. *Journal of Physiology.* 299:573–603.

Reuter, H., and H. Scholz. 1977. A study of the ion selectivity and the kinetic properties of the calcium dependent slow inward current in mammalian cardiac muscle. *Journal of Physiology.* 264:17–47.

Rios, E., and G. Brum. 1987. Involvement of dihydropyridine receptors in excitation-contraction coupling in skeletal muscle. *Nature.* 325:717–720.

Sanguinetti, M. C., and R. S. Kass. 1984. Voltage-dependent block of calcium channel current in the calf cardiac Purkinje fiber by dihydropyridine calcium channel antagonists. *Circulation Research.* 55:336–348.

Scheuer, T., and W. F. Gilly. 1986. Charge movement and depolarization-contraction coupling in arthropod vs. vertebrate skeletal muscle. *Proceedings of the National Academy of Sciences.* 83:8799–8803.

Schwartz, L. M., E. W. McCleskey, and W. Almers. 1985. Dihydropyridine receptors in muscle are voltage-dependent but most are not functional calcium channels. *Nature.* 314:747–751.

Tanguy, J., and J. Z. Yeh. QX-314 restores gating charge immobilization abolished by chloramine-T treatment in squid giant axons. *Biophysical Journal.* 56:421–427.

Uehara, A., and J. R. Hume. 1985. Interactions of organic calcium channel antagonists with calcium channels in single frog atrial cells. *Journal of General Physiology.* 85:621–647.